Hindawi
Advances in Civil Engineering
Volume 2022, Article ID 2473721, 10 pages
https://doi.org/10.1155/2022/2473721

Research Article

Simplified Calculation Method for Overlying Pipeline Deformation Induced by Tunnel Construction in Soil Based on the Energy Principle

Minghui Yang,[1,2] **Tao Yang**,[1] **and Bo Deng**[3]

[1]*College of Civil Engineering, Hunan University, Changsha 410082, Hunan, China*
[2]*Department of Civil Engineering, Xiamen University, Xiamen 361005, Fujian, China*
[3]*College of Civil Engineering, University of South China, Hengyang 421001, Hunan, China*

Correspondence should be addressed to Bo Deng; parl_d@126.com

Received 21 July 2022; Accepted 12 September 2022; Published 3 October 2022

Academic Editor: Pengjiao Jia

The deformation of the overlay pipeline caused by the excavation of the soil tunnel in the case of small spacing cannot be ignored. Based on the experience of previous engineering, this paper assumes that the settlement of the overlying pipeline caused by tunnel excavation satisfies the basic morphology of Gaussian distribution. On this basis, the soil displacement is converted into load acting on the pipeline, and the energy variation principle is introduced, and the energy variation equation of the pipe-soil system is established, which is iteratively solved based on the principle of minimum potential energy, so as to obtain the calculation method of overlay pipeline vertical deformation caused by soil tunnel excavation, which is more simple and practical than the previous method. The calculation results were compared with the existing tests and engineering examples to verify the correctness of the proposed formula. Finally, the influence of pipeline material, formation loss rate, and intersection angle between the tunnel and pipeline on pipeline vertical deformation was analyzed. The comparative analysis shows that the pipeline deformation decreases with the increase of tunnel angle and pipeline elastic modulus, but increases with the increase of formation loss rate.

1. Introduction

There are a large number of deep loess in Northwest and North China, with a maximum thickness of more than 400 meters [1], so most tunnel projects in this area do not enter the rock stratum, but cross the soil layer to form soil tunnels. In addition, due to the large number of pipeline projects such as west to east gas transmission pipeline and municipal pipeline in this region, there are many soil tunnels under the existing pipeline projects [2–4]. Compared with the rock tunnel, the excavation stability of soil tunnel is relatively poor, which may cause large deformation of the overlying soil, and then cause the disturbance of the pipeline, and even affect the normal use of the overlying pipeline in serious cases. Therefore, the reasonable calculation of the deformation value of the overlying pipeline during the excavation of the soil tunnel has become one of the most concerned issues in this type of engineering [5, 6].

For the calculation of the deformation of the overlying pipeline caused by the tunnel excavation, the commonly used methods for predicting the deflection of the pipeline mainly include theoretical calculation [7–10], numerical simulation [11–13], and model test [14–16]. Among them, the accuracy of numerical simulation depends to a large extent on the selection of soil constitutive model and parameters, and the complexity of modeling is not convenient for engineering popularization and application; however, the input of the model test is large, time-consuming, and often different from the engineering practice, which affects the prediction results. Therefore, under the

premise of the allowable accuracy of the design, according to the pipe-soil interaction model caused by tunnel excavation, the analytical approximate solution which is convenient for engineering practice is still the first choice to solve this problem.

The elastic foundation beam method and the energy variational method are common methods for analyzing the deformation of pipelines, both of which assume that the pipeline is an elastic foundation beam and its bending deformation occurs along the longitudinal direction. Among them, the former generally uses the difference method to solve the fourth-order deflection differential control equation, and the calculation process is complicated and requires more segments to achieve better calculation accuracy, which is not suitable for engineering applications. Compared with the former, the latter has the advantages of simple integral solution, no need to discretize the pipeline, and easy to achieve ideal calculation accuracy, which is convenient for popularization and application in practical engineering [17–19]. For example, Zhou et al. [20] solved the deformation of shield tunnel caused by foundation pit excavation under the effect of the faulting of lining rings based on the energy method; Zhu et al. [21] proposed a dynamic analytical model for the vibration reduction system of a floating foundation supported by elastic components based on the energy method and the Lagrange equation of motion. In terms of pipeline deformation caused by tunnel excavation, Liu et al. [22] calculated the vertical displacement of single- and double-track tunnels passing through underground pipelines based on the energy method. On this basis, Wei et al. [23] further considered the characteristics of different soils and proposed the calculation method of pipeline deformation caused by the construction of quasirectangular shield or double-circle shield. It is still slightly complicated, which limits its engineering promotion and application.

In view of this, based on the previous research results, this paper further simplifies the calculation on the basis of clarifying the basic form of soil and overlying pipeline deformation caused by tunnel excavation and puts forward a concise calculation method of pipeline deformation caused by soil tunnel excavation based on energy method and compared with the results of centrifuge test, engineering example, and existing literature. It has certain guiding significance for practical engineering.

2. Computational Models and Assumptions

Due to the complexity of the tunnel-pipe-soil interaction in the process of tunnel excavation, it is difficult to use direct modeling for analysis, and most of them use the two-stage method for approximate theoretical analysis [24, 25]. First, calculate the vertical displacement of soil caused by tunnel excavation at the pipeline axis (ignoring the influence of pipeline). On this basis, a pipe-soil interaction model is established, the soil deformation result is regarded as an external load, the obtained soil-free displacement is applied to the pipeline, the vertical load deformation balance differential equation of the pipeline is established and solved, and then an energy equation to solve for pipe deformation was constructed. For the convenience of calculation, the basic assumptions used in this paper are as follows:

(1) Both the pipeline and the soil are continuous homogeneous bodies, and the sectional dimension change caused by the pipeline deformation is ignored.

(2) The foundation under the pipeline is regarded as the Pasternak foundation, and the pipeline is regarded as a homogeneous, continuous Euler beam.

(3) The pipe and soil are always in contact, and the stratum loss remains unchanged.

2.1. Tunnel Excavation-Induced Formation Deformation Mode. According to the above ideas, the deformation of soil layer during tunnel excavation can be calculated first. From Reference [26], according to a large number of engineering examples, it is found that the stratum settlement curve perpendicular to the tunnel axis caused by ground loss during tunnel excavation roughly conforms to the following function (see in Figure 1):

$$S(x') = S_{\max} \exp\left[-\frac{(x')^2}{2i_s^2}\right], \quad S_{\max} = \frac{\pi R^2 \eta}{i_s \sqrt{2\pi}}, \tag{1}$$

where x' is the distance from the tunnel axis; $S(x')$ is the ground surface settlement at x' and $S_{\max}$ is the maximum value of ground surface settlement; η is the formation loss rate; R is the tunnel radius; and i_s is the distance from the center of symmetry of the soil settlement curve to the inflection point of the curve, which is generally called "settlement trough width." According to Jiang et al. [27], the inflection point of soil settlement curve is as follows:

$$i_s = 1.15R\left(\frac{H}{2R}\right)^{0.9}\left(1 - \frac{z_s}{H}\right)^{0.3}, \tag{2}$$

where z_s is the depth from the surface. If it is assumed that there is an angle θ between the soil profile and the tunnel axis, the Peck formula can be modified as follows:

$$S(x) = S_{\max} \exp\left[-\frac{(x \sin\theta)^2}{2i_s^2}\right]. \tag{3}$$

2.2. Pipeline Deformation Induced by Tunnel Excavation. Tunnel excavation will inevitably cause deformation of the overlying pipeline. For flexible pipelines, Zhu et al. [14] and Wang et al. [15] showed through similar indoor model test results that the deformation of the overlying pipeline is in a good agreement with the distribution of Gaussian curve during tunnel excavation. While Han et al. [7], Gu et al. [8], and Klar et al. [9] proved that the pipeline deformation mode using Gaussian distribution is more reasonable from the point of view of theoretical analysis. For this reason, the

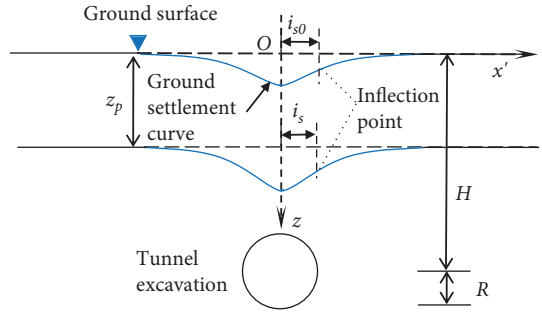

Figure 1: Soil settlement caused by tunnel excavation.

pipeline deformation model is still used in this paper, and the calculation model is shown in Figure 2, and the pipeline deformation function is as follows:

$$w(x) = A\exp\left[-\frac{x^2}{2i_p^2}\right], \tag{4}$$

where x is the distance from a point on the pipeline to the center of symmetry of the settlement curve; $w(x)$ is the vertical deformation at coordinate x on the pipeline; A is the maximum vertical deformation of the pipeline; and i_p is the distance from the center of symmetry of the pipeline settlement curve to the inflection point of the curve, which is called "pipeline settlement tank width." According to equation (4), the vertical deformation of the pipeline can be solved only if the values of A and i_p are required.

3. Solution of Pipeline Deformation by Energy Method

3.1. Construction of Energy Equation of Pipe-Soil System. Figure 3 shows the interaction between the existing pipeline and the newly excavated tunnel. The excavation of the tunnel below will inevitably lead to the release of surface stress, resulting in soil movement, and ultimately leading to the longitudinal displacement difference of the overlying pipeline. If the overlying pipeline and the soil between the tunnel and the tunnel are taken as the research system, the deformation effect of the soil above the pipeline is transformed into load acting on the pipeline, while the soil below the pipeline provides support for the pipeline, and the pipeline is placed on an elastic foundation.

Among the common foundation models, the Winkler foundation model and the Pasternak foundation model are widely used, as shown in Figure 4. The Winkler foundation is assumed to be composed of a series of continuously distributed, nonconnected discrete springs, which can give satisfactory results to many practical problems. However, the Winkler foundation cannot account for shearing between adjacent springs. Adopting the Winkler foundation will overestimate the bending moment of the elastic beam due to the discontinuity of adjacent springs [28].

If the Pasternak foundation model is used to simulate the foundation soil beneath the pipeline, according to the assumption (3) that tunnel excavation does not change the formation loss rate, then the soil settlement function and pipeline deformation function should meet the following requirements:

$$\frac{\sqrt{2\pi}i_s S_{\max}}{\sin\theta} = \sqrt{2\pi}i_p A, \tag{5}$$

$$i_{s\theta} = \frac{i_s}{\sin\theta}. \tag{6}$$

Due to the existence of pipeline, there is a difference between the vertical displacement of soil and the pipeline deformation at the axis of the pipeline, that is, the relative displacement of soil and pipe is $S_{rel} = S(x)\text{-}w(x)$, then the external force acted by soil displacement on the pipeline is as follows:

$$F = K \cdot S_{rel} - G\frac{d^2 S_{rel}}{dx^2}, \tag{7}$$

where K is the modified elastic modulus of soil, which can be calculated by the method proposed by Vesic [29] and modified by Attewell et al. [30] as follows:

$$K = \frac{1.30E}{1-\nu^2}\cdot\sqrt[12]{\frac{Ed^4}{E_p I_p}}, \tag{8}$$

where E_pI_p is the bending stiffness of pipeline, d is the pipeline diameter, ν is the soil Poisson's ratio, and E is the soil elastic modulus.

The work by the soil displacement on the pipeline can be expressed as follows:

$$\Pi_s = \frac{1}{2}\int_{-\infty}^{+\infty}(S(x)-w(x)) \cdot\left[K(S(x)-w(x)) - G\left(\frac{d^2S(x)}{dx^2}-\frac{d^2w(x)}{dx^2}\right)\right]dx, \tag{9}$$

where G is the foundation shear stiffness, which can be calculated by the value suggested by Tanahashi [28]:

$$G = \frac{Eh}{6(1+\nu)}d, \tag{10}$$

where h is the depth affected by the tunnel deformation in the Pasternak foundation model. Xu [31] suggested that h should be 2.5 times the diameter of the pipeline, that is, $h = 2.5\,d$.

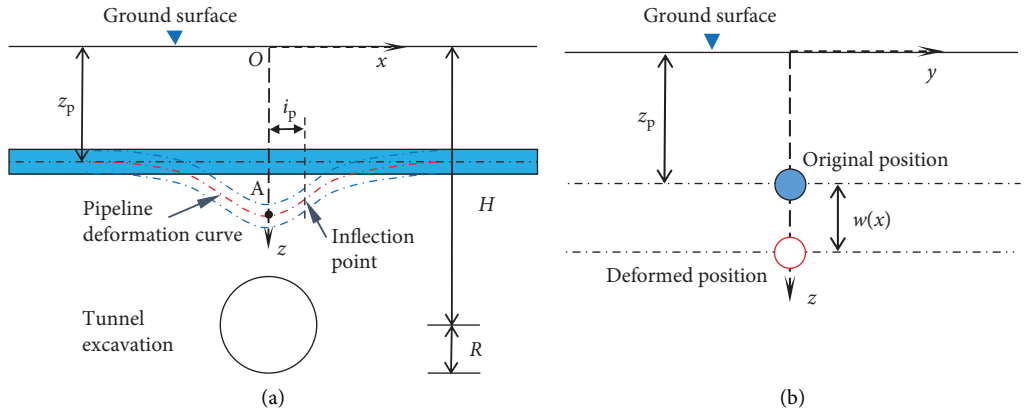

Figure 2: Deformation calculation diagram of pipeline during tunnel excavation. (a) In the x-z plan and (b) in the y-z plan.

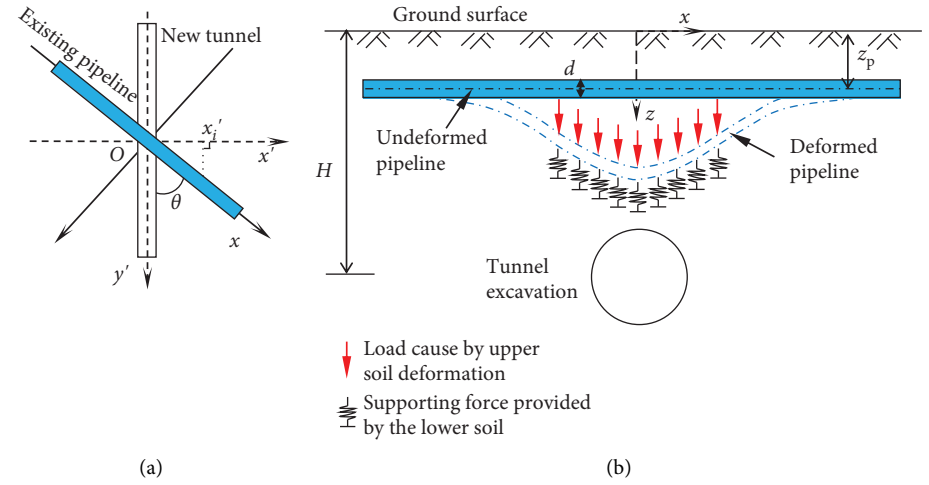

Figure 3: Deformation calculation diagram of pipeline during tunnel excavation. (a) Plan view. (b) Cross section view.

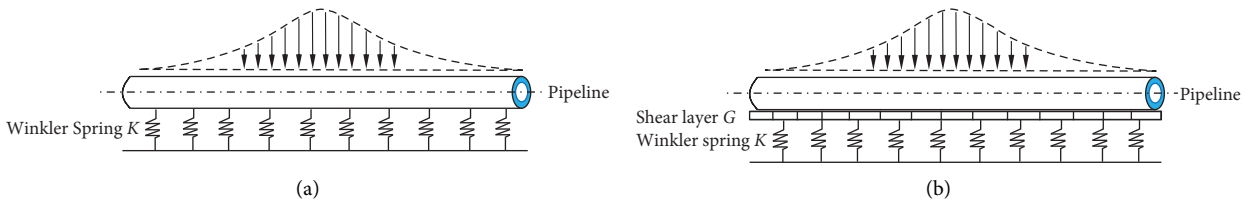

Figure 4: Two different foundation models. (a) Winkler foundation model. (b) Pasternak foundation model.

The bending strain energy of the pipeline is as follows:

$$\Pi_p = \frac{E_p I_p}{2} \int_{-\infty}^{+\infty} \left(\frac{d^2 w(x)}{dx^2} \right)^2 dx. \tag{11}$$

Then, the total potential energy of the system is $\prod = \prod_P + \prod_S$.

3.2. Pipeline Deformation Solution. According to the principle of minimum potential energy, the real displacement field of the pipe-soil system makes the total potential energy functional take the minimum value, then:

$$\frac{\delta \Pi}{\delta A} = \frac{\delta \Pi_p}{\delta A} + \frac{\delta \Pi_S}{\delta A} = 0. \tag{12}$$

Substituting equations (9) and (11) into equation (12) yields the following:

$$E_p I_p \int_{-\infty}^{+\infty} \frac{\partial^2 w(x)/\partial x^2}{\partial A} \cdot \frac{\partial^2 w(x)}{\partial x^2} \mathrm{d}x - K \int_{-\infty}^{+\infty} \frac{\partial w(x)}{\partial A} (S(x) - w(x)) \mathrm{d}x + \frac{G}{2} \int_{-\infty}^{+\infty} \frac{\partial w(x)}{\partial A} \left(\frac{d^2 S(x)}{\mathrm{d}x^2} - \frac{\partial^2 w(x)}{\partial x^2} \right) + (S(x) - w(x)) \frac{\partial^2 w(x)/\partial x^2}{\partial A} \mathrm{d}x = 0, \tag{13}$$

$$\int_{-\infty}^{+\infty} \left[\frac{\partial^2 w(x)/\partial x^2}{\partial A} \cdot \frac{\partial^2 w(x)}{\partial x^2} + \lambda \frac{\partial w(x)}{\partial A} w(x) \right] dx - \frac{\varepsilon}{2} \int_{-\infty}^{+\infty} \frac{\partial w(x)}{\partial A} \cdot \frac{\partial^2 w(x)}{\partial x^2} dx + \frac{\partial^2 w(x)/\partial x^2}{\partial A} w(x) \mathrm{d}x = \lambda \int_{-\infty}^{+\infty} \frac{\partial w(x)}{\partial A} S(x) \mathrm{d}x - \frac{\varepsilon}{2} \int_{-\infty}^{+\infty} \frac{\partial w(x)}{\partial A} \cdot \frac{d^2 S(x)}{dx^2} dx + \frac{\partial^2 w(x)/\partial x^2}{\partial A} S(x) \mathrm{d}x, \tag{14}$$

where $\lambda = K/E_{\mathrm{p}} I_{\mathrm{p}}$ and $\varepsilon = G/E_{\mathrm{p}} I_{\mathrm{p}}$.

Substituting equations (2) and (4) and (5) and (6) into equation (14) yields the following:

$$\int_{-\infty}^{+\infty} A \left(\frac{x^2}{i_p^4} - \frac{1}{i_p^2} \right)^2 \exp\left[-\frac{x^2}{i_p^2} \right] \mathrm{d}x + \lambda \int_{-\infty}^{+\infty} A \exp\left[-\frac{x^2}{i_p^2} \right] \mathrm{d}x - \varepsilon \int_{-\infty}^{+\infty} A \left(\frac{x^2}{i_p^4} - \frac{1}{i_p^2} \right) \exp\left[-\frac{x^2}{i_p^2} \right] \mathrm{d}x = \lambda \int_{-\infty}^{+\infty} \mathrm{S}_{\max} \exp\left[-\left(\frac{1}{2i_p^2} + \frac{1}{2i_{s\theta}^2} \right) x^2 \right] dx - \frac{\varepsilon}{2} \int_{-\infty}^{+\infty} \mathrm{S}_{\max} \left[\left(\frac{1}{i_{s\theta}^4} + \frac{1}{i_p^4} \right) x^2 - \left(\frac{1}{i_{s\theta}^2} + \frac{1}{i_p^2} \right) \right] \exp\left[-\left(\frac{1}{2i_{\mathrm{p}}^2} + \frac{1}{2i_{s\theta}^2} \right) x^2 \right] \mathrm{d}x. \tag{15}$$

Since equation (15) is difficult to calculate directly, it is first expressed separately as follows, and then integrated and simplified, respectively:

$$\int_{-\infty}^{+\infty} A \left(\frac{x^2}{i_p^4} - \frac{1}{i_p^2} \right)^2 \exp\left[-\frac{x^2}{i_p^2} \right] \mathrm{d}x = \frac{3\sqrt{\pi} A}{4 i_p^3}, \tag{16}$$

$$\lambda \int_{-\infty}^{+\infty} A \exp\left[-\frac{x^2}{i_p^2} \right] \mathrm{d}x = \lambda A \sqrt{\pi} i_p, \tag{17}$$

$$-\varepsilon \int_{-\infty}^{+\infty} A \left(\frac{x^2}{i_p^4} - \frac{1}{i_p^2} \right) \exp\left[-\frac{x^2}{i_p^2} \right] \mathrm{d}x = \frac{\sqrt{\pi} \varepsilon A}{2 i_p}, \tag{18}$$

$$\lambda \int_{-\infty}^{+\infty} \mathrm{S}_{\max} \exp\left[-\left(\frac{1}{2i_p^2} + \frac{1}{2i_{s\theta}^2} \right) x^2 \right] \mathrm{d}x = \frac{\sqrt{2\pi} \lambda \mathrm{S}_{\max} i_p i_{s\theta}}{\sqrt{i_p^2 + i_{s\theta}^2}}, \tag{19}$$

$$-\frac{\varepsilon}{2}\int_{-\infty}^{+\infty} S_{\max}\left[\left(\frac{1}{i_{s\theta}^4}+\frac{1}{i_p^4}\right)x^2-\left(\frac{1}{i_{s\theta}^2}+\frac{1}{i_p^2}\right)\right]\exp\left[-\left(\frac{1}{2_{\mathrm{ip}}^2}+\frac{1}{2\mathrm{i}_{s\theta}^2}\right)x^2\right]\mathrm{d}x=\frac{\sqrt{2\pi}\varepsilon S_{\max} i_p i_{s\theta}}{\left(i_{s\theta}^2+i_p^2\right)^{1.5}}. \tag{20}$$

Substituting equations (5) and (16)-(20) into equation (15) yields the following:

$$\frac{3}{4}\frac{1}{i_p^4}+\lambda+\frac{\varepsilon}{2i_p^2}=\frac{\sqrt{2}\left(\lambda i_{s\theta}^2+\varepsilon\right)}{\left(i_p^2+i_{s\theta}^2\right)^{1.5}}i_p+\frac{\sqrt{2}\lambda}{\left(i_p^2+i_{s\theta}^2\right)^{1.5}}i_p^3. \tag{21}$$

Equation (21) is relatively complex and difficult to solve directly. Therefore, this paper establishes the following iterative formula to solve i_{p}:

$$i_p=\left[\frac{\left(i_p^2+i_s^2/sin^2\theta\right)^{1.5}}{4\sqrt{2}\,\lambda}\left(3+4\lambda i_p^4+2\varepsilon i_p^2\right)-\left(\frac{i_s^2}{sin^2\theta}+\frac{\varepsilon}{\lambda}\right)i_p^5\right]^{1/7}. \tag{22}$$

If the Winkler foundation model is used to simulate the foundation soil beneath the pipeline, it is only necessary to substitute $\varepsilon=0$ into equation (21), then equation (22) degenerates into:

$$i_p=\frac{1}{\sqrt{2}}\left[\frac{3+4\lambda i_p^4}{\lambda\sin\theta}\sqrt{i_s^2+\left(i_p\sin\theta\right)^2}\right]^{1/5}, \tag{23}$$

where θ is the angle between pipeline and tunnel. The author suggests that the initial iteration value should be $i_{\mathrm{p0}}=(2\sim3)R$, so as to quickly obtain the final iteration value.

The parameters i_{p} and A are obtained by solving simultaneous equations (5) and (16) to complete the calculation of pipeline deformation.

4. Example Verification

4.1. Comparison with Field Measured Data. Ma [32] provided the measured data of shield tunnel excavation in a certain section of the Shenzhen metro project (the Phase 1). This section of the tunnel is located in gravelly clay and sandy clay, which is a typical soil tunnel. The comparison calculation parameters are as follows: the tunnel depth $H=14.4$ m, the tunnel diameter $D=6$ m, the pipeline diameter $d=3$ m, the pipeline wall thickness $t=0.12$ mm, the pipeline elastic modulus $E_{\mathrm{p}}=25$ GPa, the pipeline depth $z_{\mathrm{p}}=8.7$ m, the formation loss rate $\eta=0.77\%$, the soil elastic modulus $E=8.2$ MPa, the soil Poisson's ratio $v=0.3$, the bending stiffness of pipeline $E_{\mathrm{p}}I_{\mathrm{p}}=2.819\times10^{10}\mathrm{N\,m^2}$, and the tunnel is orthogonal to the pipeline, that is, $\theta=90$ degree.

The comparison between the calculated results and the measured values using equations (22) and (23) is shown in Figure 5. The measured average maximum settlement value of the pipeline is 8.30 mm, and the maximum settlement values calculated based on the Pasternak foundation and Winkler foundation are 8.63 mm and 8.55 mm, respectively. The deviations between the two foundation models and the measured values are 3.98% and 3.01%, respectively. It can be seen that the calculation method in this paper is basically consistent with the measured results, while the Pasternak foundation is slightly larger than the Winkler foundation, but the difference is small.

4.2. Comparison with the Centrifuge Test. Marshall et al. [5] measured the vertical deformation of the pipeline caused by tunnel excavation under the condition of centrifugal acceleration of 75 g. Select $\eta=0.5\%$, 1% for analysis, the main calculation parameters are as follows: the tunnel depth $H=13.65$ m, the tunnel diameter $D=4.65$ m, the diameters of the two pipelines $d=2.6$ m and 0.66 m, the bending stiffness of pipeline EpIp = 2.56 × 1010 N m2, 2.04 × 108N·m2, and the pipeline depth $z_{\mathrm{p}}=5.6$ m. The soil elastic modulus $E=19.52$ MPa, the soil Poisson's ratio $v=0.4$, the test soil sample is dry sand, and the tunnel is orthogonal to the pipeline, that is, $\theta=90$ degree

For pipelines with small stiffness, the comparison between calculation results and test values by using the formula in this paper is shown in Figure 6(a), Case 1: the formation loss rate $\eta=0.5\%$, the maximum deformation measured in the test is 5.25 mm, the maximum deformation calculated based on Pasternak foundation is 5.574 mm, while the maximum deformation calculated based on Winkler foundation is 5.573 mm, and the deviations between the calculated results and the measured values of the two foundation models are 6.17% and 5.80%, respectively; Case 2: the formation loss rate $\eta=1\%$, the maximum deformation measured in the test is 11.25 mm, the maximum deformation calculated based on Pasternak foundation is 11.148 mm, while the maximum deformation calculated based on Winkler foundation is 11.147 mm, and the deviations between the calculated results and the measured values of the two foundation models are −0.907% and −0.915%, respectively.

For pipelines with large stiffness, the comparison between calculation results and test values by using the formula in this paper is shown in Figure 6(b), Case 3: the formation loss rate $\eta=0.5\%$, the maximum settlement measured in the test is 4.5 mm, the maximum deformation calculated based on Pasternak foundation is 3.984 mm, while the maximum settlement calculated based on Winkler foundation is 3.959 mm, and the deviations between the calculated results and the measured values of the two foundation models are −11.47% and −12.02%, respectively; Case 4: the formation loss rate $\eta=1\%$, the maximum deformation measured in the test is 7.5 mm, the maximum deformation calculated based on Pasternak foundation is 7.97 mm, while the maximum deformation calculated based on Winkler foundation is 7.92 mm, and the deviations between the calculated results and the measured values of the two foundation models are 6.27% and 5.60%, respectively. In conclusion, the pipeline settlement calculated by the method in this paper is in a good agreement with the experimental values, and there is little

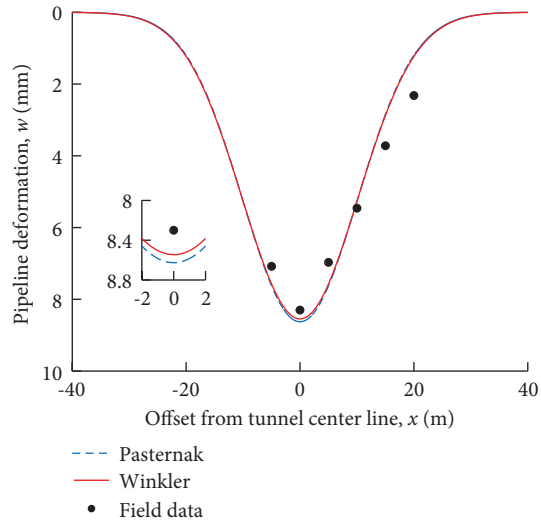

Figure 5: Comparison of analytical solution against field data.

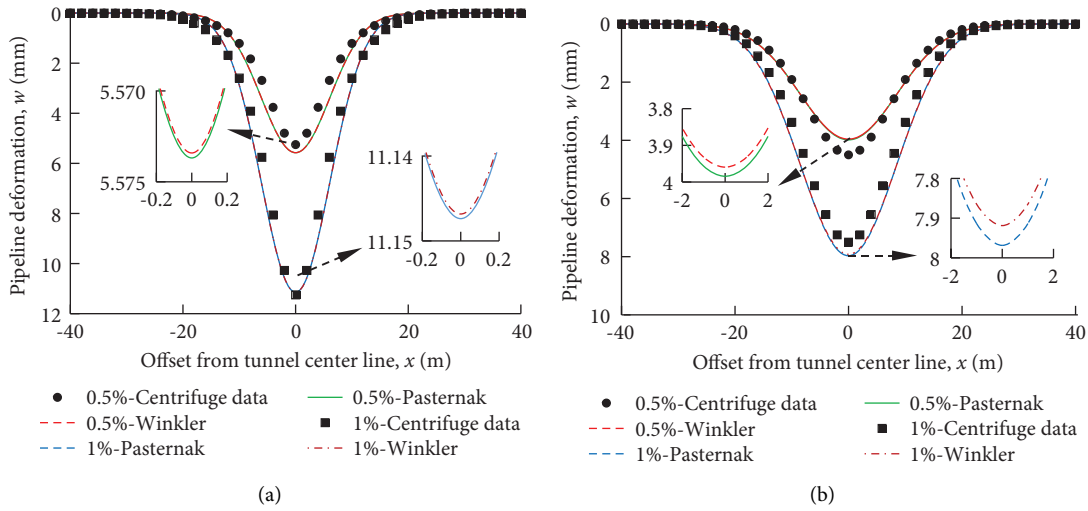

Figure 6: Comparison of analytical solution against centrifuge test data. (a) Small stiffness pipeline and (b) large stiffness pipeline.

difference in the pipeline deformation calculated by the two foundation modes for large and small stiffness pipelines.

4.3. Compared with the Existing Literature. Compared with the calculation method of Vorster et al. [33], the calculation parameters are as follows: the tunnel depth $H = 5$ m, the excavation diameter $D = 1.5$ m, the pipeline diameter $d = 0.8$ m, the bending stiffness of pipeline $E_pI_p = 1.05 \times 108$ N m2, the pipeline depth $z_p = 1.5$ m, the soil elastic modulus $E = 14.32$ MPa, the soil Poisson's ratio $v = 0.25$, and the tunnel is orthogonal to the pipeline, that is, $\theta = 90^{\circ}$. Vorster et al. [33] gave the maximum settlement value of free soil displacement Smax = 13.6 mm, and the inflection point of settlement trough is = 2.6 m in the buried depth of the pipeline.

The calculated results are shown in Figure 7. In this paper, the maximum settlement of pipeline is calculated by using Pasternak foundation and Winkler foundation as 11.93 mm and 11.89 mm, respectively. The maximum value of pipeline settlement calculated by Vorster et al. is 12 mm, and the difference between the results calculated by Pasternak foundation and Vorster et al. is −0.583%, and the difference between the results calculated by Winkler foundation and Vorster et al. is −0.917%.

5. Parametric Studies

According to the influencing factors of pipeline deformation, the factors such as pipeline material, formation loss rate, and pipe-tunnel intersection angle are analyzed. The selected calculation parameters are as follows: buried depth of tunnel axis $H = 15$ m, the tunnel diameter $D = 6$ m, the

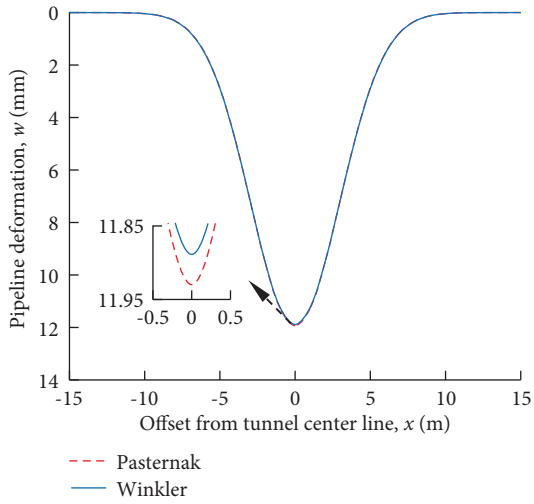

Figure 7: Comparison of analytical solution and other method.

pipeline diameter $d = 2$ m, and the pipeline wall thickness $t = 0.12$ mm. The soil elastic modulus $E = 15$ MPa and the soil Poisson's ratio $v = 0.3$. To simplify the calculation, only Pasternak foundation model calculation is used as an example in the parameter analysis.

5.1. Pipeline Material. When the buried depth of the pipeline axis is selected to be 3 m, which corresponds to the distance between the axis of the pipe and the tunnel is 12 mm, the angle between the tunnel and the pipeline $\theta = 90$ degree, and the formation loss rate $\eta = 2\%$, the commonly used pipeline material parameters are shown in Table 1.

The calculation results of pipeline deformation for different pipeline materials are shown in Figure 8. It can be seen from the figure that as the stiffness of the pipeline increases, the maximum deformation value of the pipeline decreases gradually, while the width of the pipeline settlement tank increases gradually.

5.2. Formation Loss Rate. The cast iron material in Table 1 is selected to analyze the influence of formation loss rate on pipeline deformation, and the intersection angle between the tunnel and the pipeline $\theta = 90$ degree, and the formation loss rate $\eta = 1\%$, 2%, and 3%. The calculation results are shown in Figure 9. It can be found from the figure that the maximum settlement value of the pipeline gradually increases with the increase of the formation loss rate, but the width of the pipeline settlement tank remains unchanged, indicating that the formation loss rate has a significant impact on the pipeline deformation.

5.3. Intersection Angle. Selecting the formation loss rate $\eta = 2\%$ and the cast iron pipe in Table 1, the calculation results of pipeline deformation under different tunnel intersection angles between the tunnel and the pipeline (e.g., 90 degree, 60 degree, and 30 degree) are shown in Figure 10. It can be seen from the figure that as the angle between the tunnel and the pipeline decreases, the maximum deformation value of the pipeline gradually increases, and as the angle between the tunnel and the pipeline decreases, the problem is gradually transformed into a plane problem and the corresponding maximum value of pipeline deformation gradually approached the maximum value of soil settlement. In addition, when the intersection angle between the tunnel and the pipeline changes from 90 degree to 60 degree, the increase in the maximum settlement of the soil is less than that when the angle changes from 60 degree to 30 degree. To

Table 1: Material parameters of different pipelines.

Material name	Elastic modulus (GPa)	Bending stiffness
PVC pipe	3	9.432×10^8 N·m^2
Concrete pipe	25	7.860×10^9 N·m^2
Cast iron pipe	150	4.716×10^{10} N·m^2
Steel pipe	210	6.602×10^{10} N·m^2

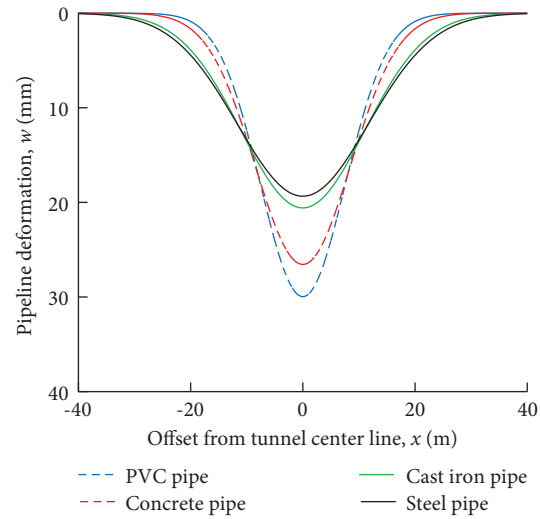

Figure 8: Pipeline deformation under different pipeline materials.

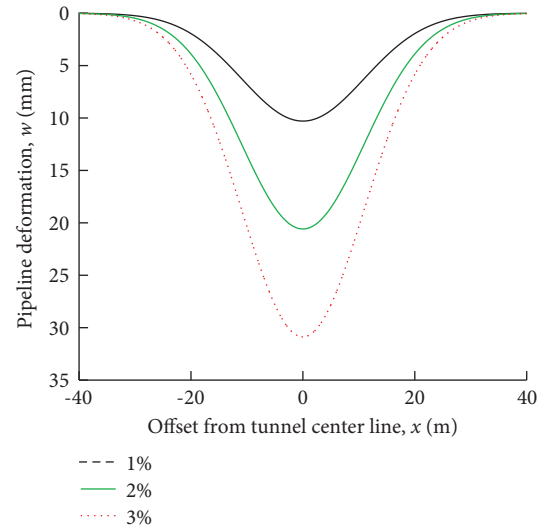

Figure 9: Pipeline deformation under different formation loss rates.

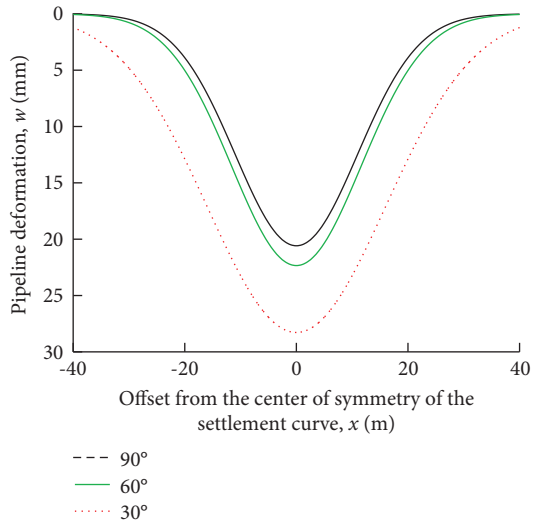

Figure 10: Pipeline deformation under different intersection angles.

speak it simply, the width of the pipe settlement tank gradually increases with the decrease of the intersection angle between the pipe and tunnel. When the intersection angle between the pipe and tunnel is close to 90 degree, the calculation as 90 degree can meet the accuracy requirements, but when the intersection angle between the pipe and tunnel is far away from 90 degree, the intersection angle between the pipe and tunnel cannot be ignored.

6. Conclusion

For the special condition of soil tunnel under the existing pipeline, this paper proposes a calculation method of pipeline deformation based on the principle of minimum potential energy based on the previous test experience. The effectiveness of the method in this paper is verified by comparison with engineering examples and centrifuge test results, and the influencing factors of pipeline deformation are analyzed. The main conclusions are as follows:

(1) As the stiffness of the pipeline increases, the maximum settlement value of the pipeline gradually decreases, while the width of the deformation trough gradually increases.

(2) With the increase of formation loss rate, the maximum deformation value of pipeline increases gradually, but the width of the pipeline settlement tank remains unchanged.

(3) With the decrease of the angle between the tunnel and the pipeline, the maximum deformation of the pipeline increases gradually, and the width of the pipeline settlement tank increases gradually.

Data Availability

The data used to support the findings of this study are included within the article.

Conflicts of Interest

The authors declare that they have no conflicts of interest.

Acknowledgments

This research was supported by the Transportation Science and Technology Project of Henan Province (2019J-2-12, 2021J7) and Science Foundation for Youths of Hunan Province of China (2021JJ40460), which are gratefully acknowledged.

References

[1] Z. J. Xue, Z. G. Lin, and M. S. Zhang, "Loess in China and loess landslides," *Chinese Journal of Rock Mechanics and Engineering*, vol. 26, no. 7, pp. 1297–1312, 2007, in Chinese.

[2] L. Zhang, X. Wu, Y. Qin, M. J. Skibniewski, and W. Liu, "Towards a fuzzy Bayesian network based approach for safety risk analysis of tunnel-induced pipeline damage," *Risk Analysis*, vol. 36, no. 2, pp. 278–301, 2016.

[3] Y. K. Sun, W. Y. Wu, and T. Q. Zhang, "Analysis on the pipeline settlement in soft ground induced by shield tunneling across buried pipeline," *China Railway Science*, vol. 30, no. 1, pp. 80–85, 2009, in Chinese.

[4] N. Jiang, T. Gao, C. Zhou, and X. Luo, "Effect of excavation blasting vibration on adjacent buried gas pipeline in a metro tunnel," *Tunnelling and Underground Space Technology*, vol. 81, pp. 590–601, 2018.

[5] A. M. Marshall, A. Klar, and R. J. Mair, "Tunneling beneath buried pipes: view of soil strain and its effect on pipeline behavior," *Journal of Geotechnical and Geoenvironmental Engineering*, vol. 136, no. 12, pp. 1664–1672, 2010.

[6] A. Klar, "Elastic continuum solution for tunneling effects on buried pipelines using fourier expansion," *Journal of Geotechnical and Geoenvironmental Engineering*, vol. 144, no. 9, Article ID 4018062, 2018.

[7] X. Han, C. H. Lei, and P. Zhang, "A modified stiffness approach to predict tunnelling induced deformation and force of pipelines," *Journal of Civil & Environmental Engineering*, vol. 34, no. 3, pp. 21–27, 2012, in Chinese.

[8] S. C. Gu, H. W. He, and G. F. Ru, "Analysis of underground pipeline stress caused by metro tunneling," *Urban Mass Transit*, vol. 5, pp. 14–18, 2015, in Chinese.

[9] A. Klar and A. M. Marshall, "Linear elastic tunnel pipeline interaction: the existence and consequence of volume loss equality," *Géotechnique*, vol. 65, no. 9, pp. 788–792, 2015.

[10] C. Lin, M. Huang, F. Nadim, and Z. Liu, "Tunnelling-induced response of buried pipelines and their effects on ground settlements," *Tunnelling and Underground Space Technology*, vol. 96, Article ID 103193, 2020.

[11] Y. Wang, J. Shi, and C. W. W. Ng, "Numerical modeling of tunneling effect on buried pipelines," *Canadian Geotechnical Journal*, vol. 48, no. 7, pp. 1125–1137, 2011.

[12] M. Xu and L. Shi, "A Numerical study on the effect of tunneling on adjacent buried pipelines," in *Proceedings of the International Conference on Pipelines and Trenchless Technology*, pp. 1376–1387, Beijing, China, October 2011.

[13] J. Shi, Y. Wang, and C. W. W. Ng, "Numerical parametric study of tunneling-induced joint rotation angle in jointed pipelines," *Canadian Geotechnical Journal*, vol. 53, no. 12, pp. 2058–2071, 2016.

[14] Y. T. Zhu, H. Zhang, Z. X. Zhang, X. Huang, and K. Liu, "Physical model test study of influence of advance of shield

tunnel on adjacent underground pipelines," *Rock and Soil Mechanics*, vol. 37, no. 2, pp. 151–160, 2016, in Chinese.

[15] H. T. Wang, H. Jin, and D. J. Yuan, "Model test study on influence of pipeline caused by tunnel construction in sand," *China Civil Engineering Journal*, vol. 50, no. 2, pp. 118–126, 2017, in Chinese.

[16] S. Ma, Y. Shao, Y. Liu, J. Jiang, and X. Fan, "Responses of pipeline to side-by-side twin tunnelling at different depths: 3D centrifuge tests and numerical modelling," *Tunnelling and Underground Space Technology*, vol. 66, pp. 157–173, 2017.

[17] J. L. Figueroa, A. S. Saada, L. Liang, and N. M. Dahisaria, "Evaluation of soil liquefaction by energy principles," *Journal of Geotechnical Engineering*, vol. 120, no. 9, pp. 1554–1569, 1994.

[18] M. Z. Chen, X. N. Gong, and J. X. Ying, "Variational solution for pile group–pile cap (raft)," *China Civil Engineering Journal*, vol. 34, no. 6, pp. 67–73, 2001, in Chinese.

[19] H. S. Shang, H. Zhang, and F. Y. Liang, "Lateral bearing capacity of pile foundation due to shallow tunneling," *Chinese Journal of Geotechnical Engineering*, vol. 35, no. z2, pp. 740–743, 2013, in Chinese.

[20] S. H. Zhou, J. H. Xiao, and C. He, "Energy method for calculating deformation of adjacent shield tunnels due to foundation pit excavation considering step between rings," *China Railway Science*, vol. 37, no. 3, pp. 53–60, 2016, in Chinese.

[21] L. J. Zhu, L. H. Wen, and S. Hei, "Analytical model of floating foundation vibration reduction system based on energy method," *Earthquake Engineering and Engineering Dynamics*, vol. 42, no. 2, pp. 104–112, 2022, in Chinese.

[22] X. Q. Liu, F. Y. Liang, H. Zhang, and F. Chu, "Energy variational solution for settlement of buried pipeline induced by tunneling," *Rock and Soil Mechanics*, vol. 35, no. 2, pp. 217–222, 2014, in Chinese.

[23] G. Wei, C. H. Cui, and X. Xu, "Calculation of pipeline settlement induced by double-o-tube shield tunneling based on energy method," *Chinese Journal of Underground Space and Engineering*, vol. 15, no. 4, pp. 1106–1111, 2019, in Chinese.

[24] A. Klar, T. E. B. Vorster, K. Soga, and R. J. Mair, "Soil—pipe interaction due to tunnelling: comparison between Winkler and elastic continuum solutions," *Géotechnique*, vol. 55, no. 6, pp. 461–466, 2005.

[25] H. Zhang and Z. X. Zhang, "Vertical deflection of existing pipeline due to shield tunnelling," *Journal of Tongji University*, vol. 41, no. 8, pp. 1172–1178, 2013, in Chinese.

[26] R. B. Peck, "Deep excavations and tunnelling in soft ground," in *Proceedings of the 7th International Conference on soil Mechanics and Foundation Engineering*, pp. 225–290, Mexico, 1969.

[27] X. L. Jiang, Z. M. Zhao, and Y. Li, "Analysis and calculation of surface and subsurface settlement trough profiles due to tunneling," *Rock and Soil Mechanics*, vol. 25, no. 10, pp. 1542–1544, 2004, in Chinese.

[28] H. Tanahashi, "Formulas for an infinitely long Bernoulli-Euler beam on the Pasternak model," *Soils and Foundations*, vol. 44, no. 5, pp. 109–118, 2004.

[29] A. B. Vesic, "Bending of beams Resting on Isotropic elastic Solid," *Journal of the Engineering Mechanics Division*, vol. 87, no. 2, pp. 35–53, 1961.

[30] P. B. Attewell, J. Yeates, and A. R. Selby, *Soil Movements Induced by Tunnelling and Their Effects on Pipelines and Structures*, Blackie & Son, London, UK, 1986.

[31] L. Xu, *Study on Longitudinal Settlement of Soft Soil Shield Tunnel*, Tongji University, Shanghai, China, 2005, in Chinese.

[32] T. Ma, *The Research of Tunneling- Induced Ground Surface Movements and Their Influence to Adjacent Utilities*, Changsha University of Science & Technology, Changsha, China, 2005, in Chinese.

[33] T. E. Vorster, A. Klar, K. Soga, and R. J. Mair, "Estimating the effects of tunneling on existing pipelines," *Journal of Geotechnical and Geoenvironmental Engineering*, vol. 131, no. 11, pp. 1399–1410, 2005.